

Figure S1. Quantitative cellular uptake of ginsenoside liposomes with different glucose transporter (GLUT) inhibitors (n = 3; mean \pm standard deviation).

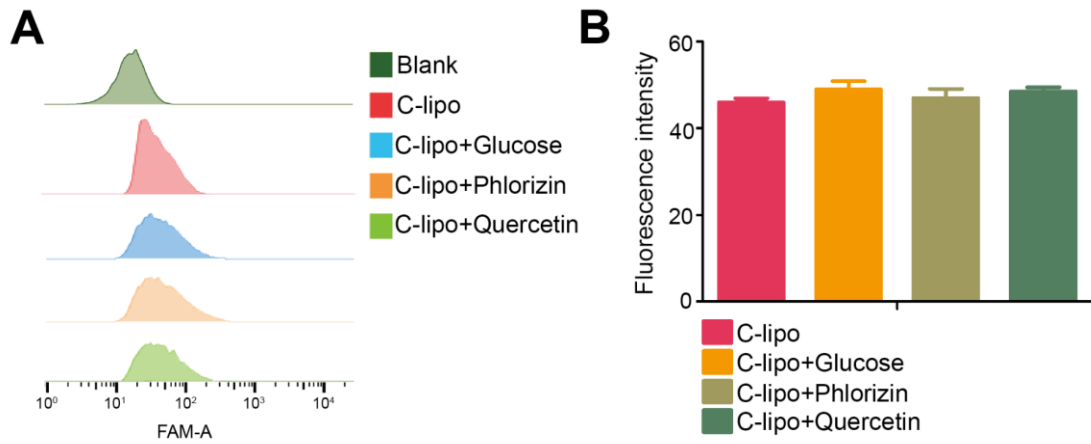


Figure S2. Quantitative cellular uptake of C-lipo with different GLUT inhibitors (n = 3; mean ± standard deviation).

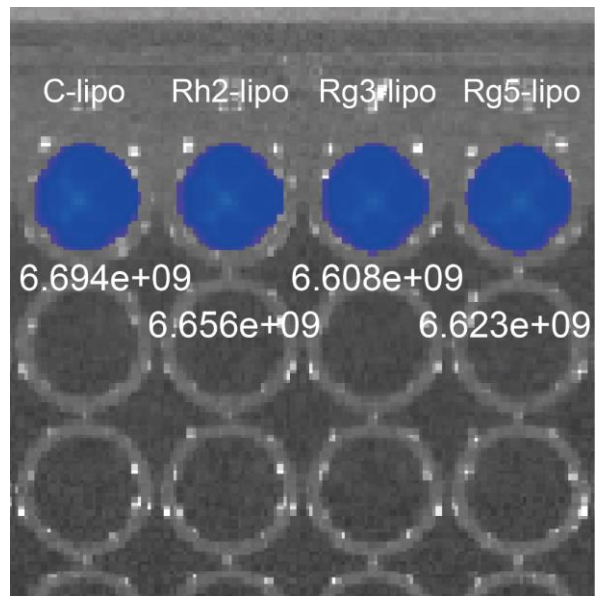


Figure S3. The same injection dose of 1,1'-dioctadecyl-3,3',3'-tetramethylindotricarbocyanineiodide loaded liposomes were given to mice for *in vivo* targeting imaging.

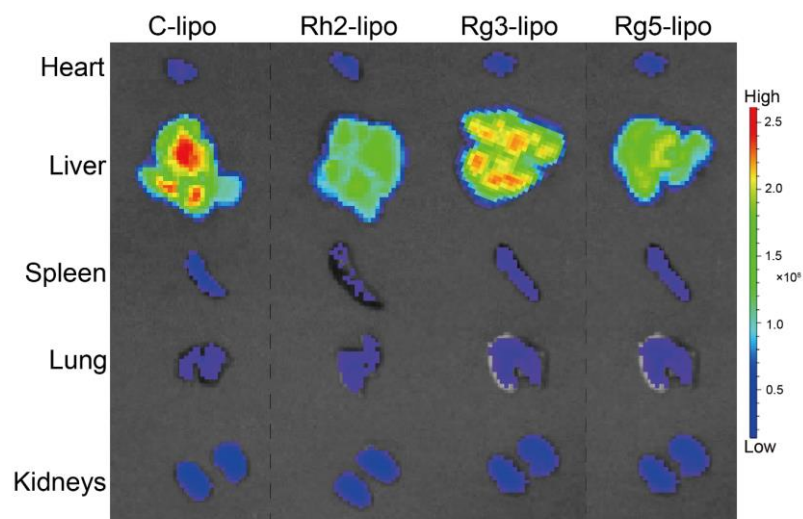


Figure S4. Fluorescent images of dissected organs of mice sacrificed after 24 h.

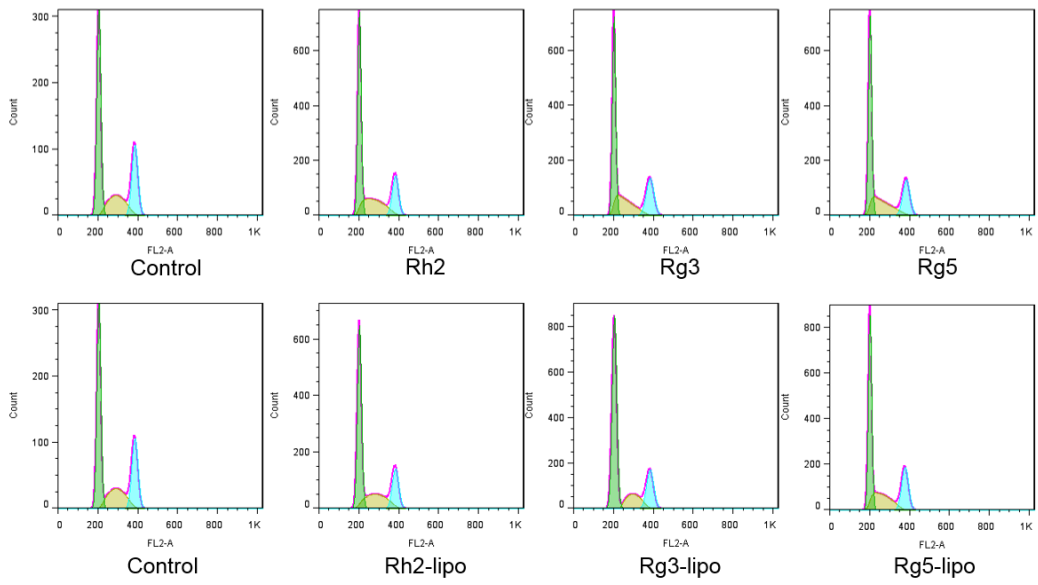


Figure S5. Cell cycle of BGC-823 cells treated with different ginsenoside liposomes and free ginsenosides, analyzed by flow cytometry.

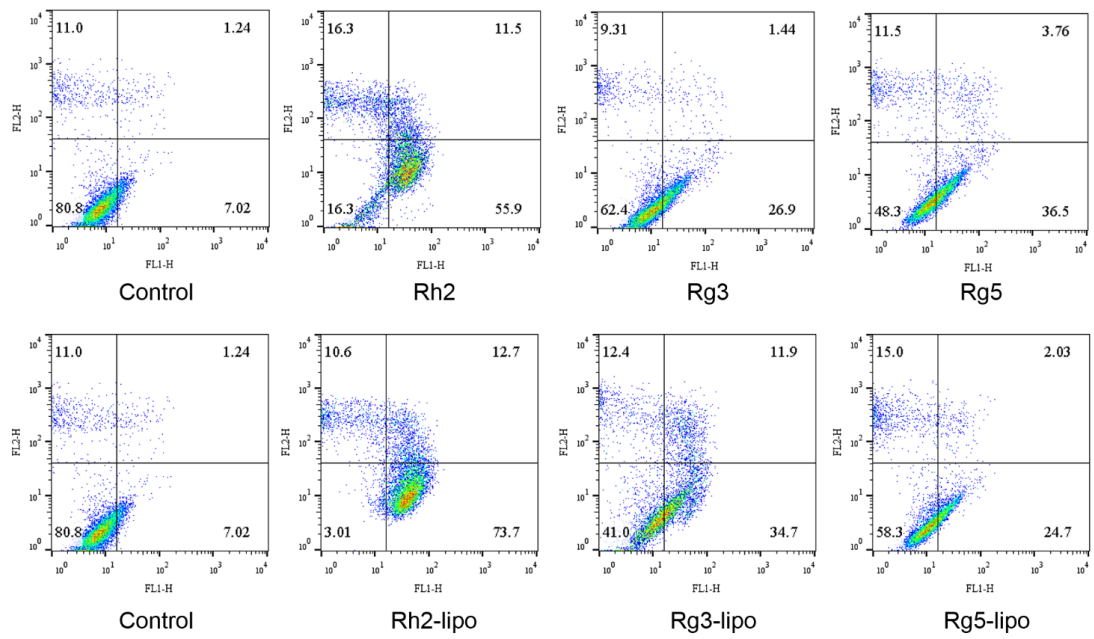


Figure S6. Apoptosis induced by different ginsenoside liposomes and free ginsenosides in BGC-823 cells, measured by flow cytometry.

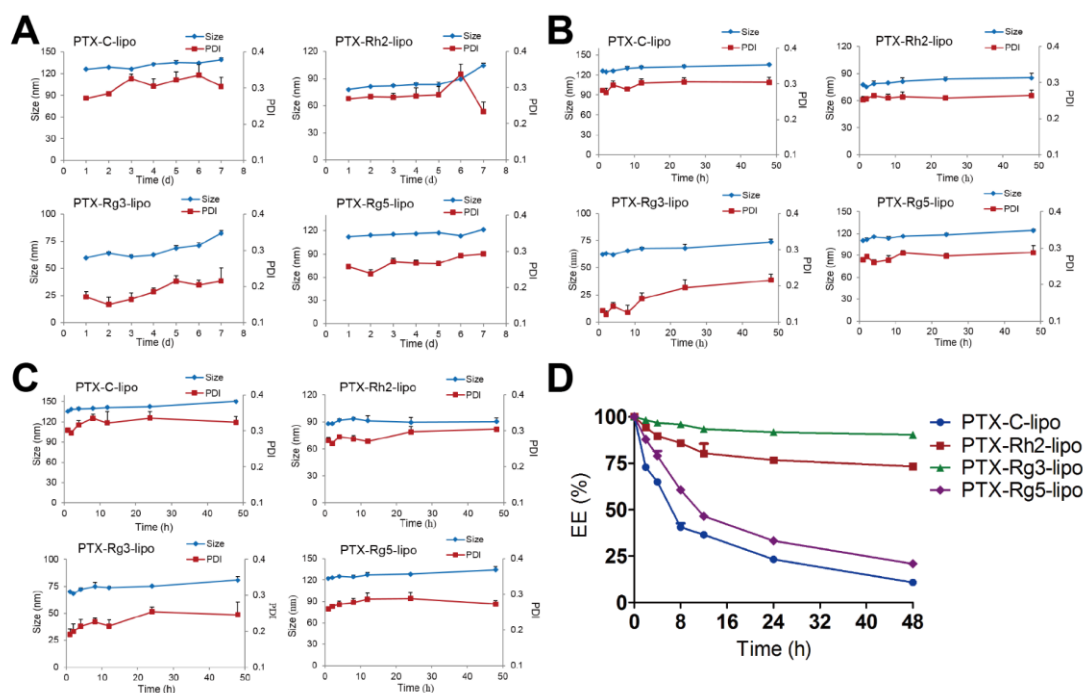


Figure S7. Change in size and polydispersity index of different paclitaxel (PTX)-loaded liposomal formulations in PBS at 4 °C (A) and 37 °C (B) or in 10% fetal bovine serum (C) (n = 3; mean ± standard deviation [SD]). (D) Drug leakage profiles of PTX-loaded liposomal formulations (n = 3; mean ± SD).

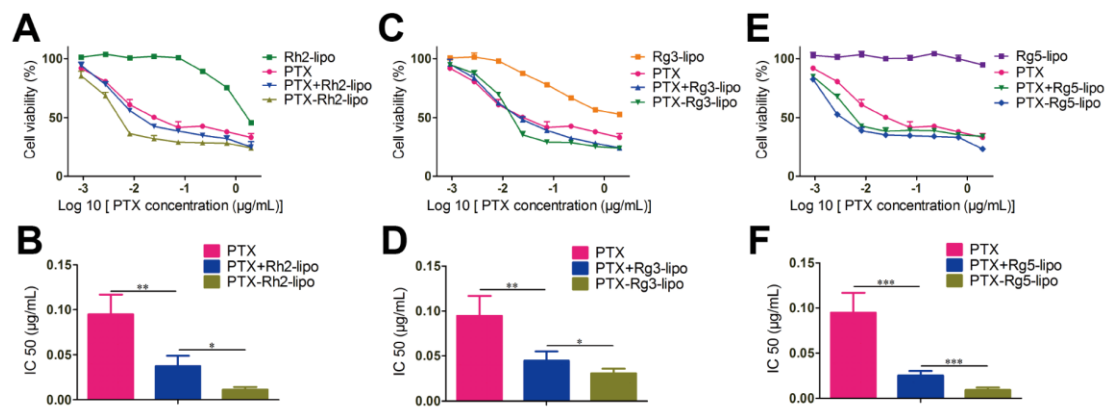


Figure S8. Cytotoxicity (A, C, E) and IC₅₀ values (B, D, F) of free paclitaxel (PTX), physical mixture of free PTX and blank ginsenoside liposomes, and different types of PTX-loaded liposomes in BGC-823 cells (n = 6; mean ± standard deviation).

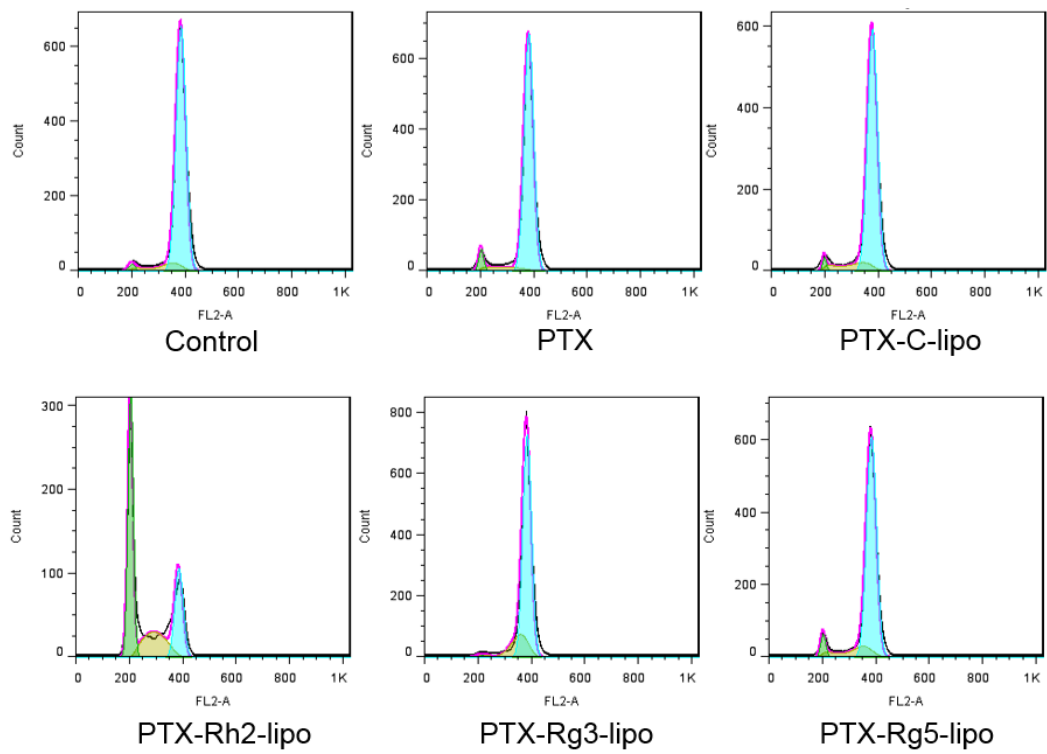


Figure S9. Cell cycle of BGC-823 cells treated with free paclitaxel (PTX) and different PTX-loaded liposomes, measured by flow cytometry.

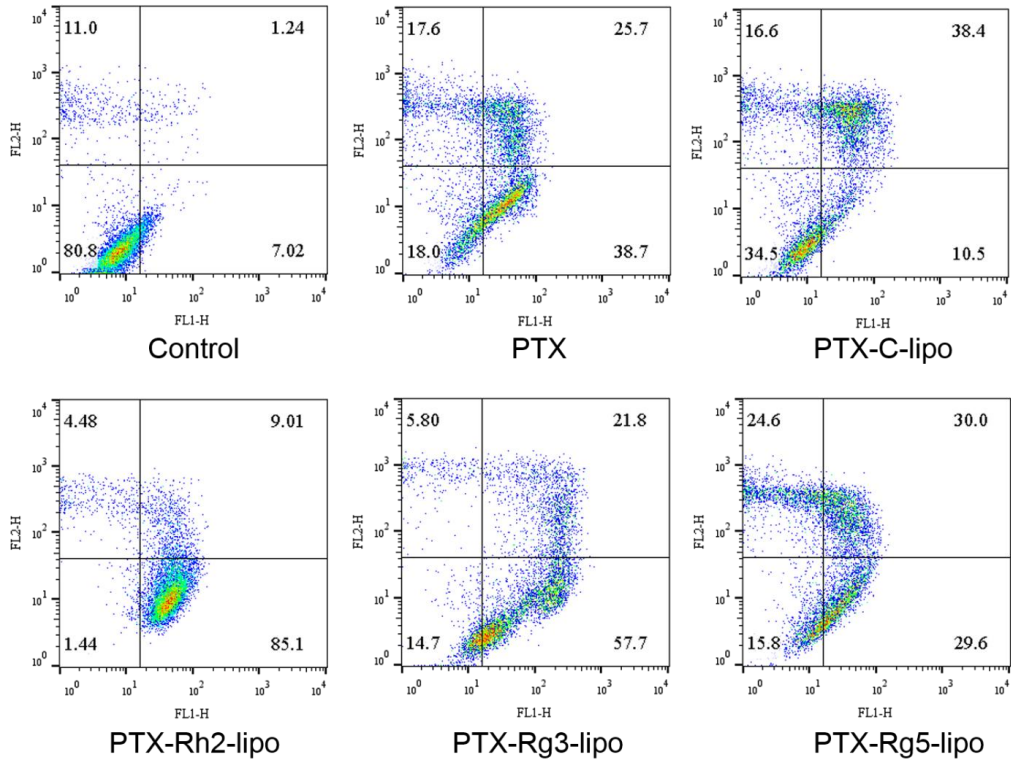


Figure S10. Cell apoptosis induced by free paclitaxel (PTX) and different PTX-loaded liposomes, measured by flow cytometry.